Neuron
Report

# Rapid Synaptic Scaling Induced by Changes in Postsynaptic Firing

Keiji Ibata,[1,2,3] Qian Sun,[1,3] and Gina G. Turrigiano[1,*]
[1]Department of Biology and Center for Behavioral Genomics, Brandeis University, Waltham, MA 02454, USA
[2]Present address: Laboratory for Cell Function Dynamics, Brain Science Institute, The Institute of Physical and Chemical Research (RIKEN), 2-1 Hirosawa, Wako-shi, Saitama, 351-0198, Japan.
[3]These authors contributed equally to this work.
*Correspondence: turrigiano@brandeis.edu
DOI 10.1016/j.neuron.2008.02.031

## SUMMARY

**Homeostatic synaptic scaling adjusts a neuron's excitatory synaptic strengths up or down to compensate for perturbations in activity. Little is known about the molecular pathway(s) involved, nor is it clear which aspect of "activity"—local synaptic signaling, postsynaptic firing, or large-scale changes in network activity—is required to induce synaptic scaling. Here, we selectively block either postsynaptic firing in individual neurons or a fraction of presynaptic inputs, while optically monitoring changes in synaptic strength. We find that synaptic scaling is rapidly induced by block of postsynaptic firing, but not by local synaptic blockade, and is mediated through a drop in somatic calcium influx, reduced activation of CaMKIV, and an increase in transcription. Cortical neurons thus homeostatically adjust synaptic strengths in response to changes in their own firing rate, a mechanism with the computational advantage of efficiently normalizing synaptic strengths without interfering with synapse-specific mechanisms of information storage.**

## INTRODUCTION

Storage of memories and the activity-dependent refinement of neuronal circuitry are thought to require two distinct forms of synaptic plasticity; synapse-specific mechanisms that selectively alter the strength of particular connections (Malenka and Bear, 2004) and homeostatic mechanisms such as synaptic scaling that regulate the overall strength of a neuron's synaptic inputs (Abbott and Nelson, 2000; Turrigiano and Nelson, 2004). Synaptic scaling has now been well documented at a variety of central synapses (Burrone and Murthy, 2003; Turrigiano and Nelson, 2004) and also occurs in vivo in response to developmental or activity-dependent changes in sensory input (Desai et al., 2002; Goel et al., 2006; Maffei et al., 2004), suggesting that it plays an important role in the developmental refinement of neuronal circuitry.

There is good consensus that a major expression locus of synaptic scaling is changes in the synaptic accumulation of AMPA-type glutamate receptors (Grunwald et al., 2004; Ju et al., 2004; Lissin et al., 1998; O'Brien et al., 1998; Thiagarajan et al., 2005; Turrigiano et al., 1998; Wierenga et al., 2005). In contrast, much less is known about how synaptic scaling is induced. Several signaling molecules have been suggested to mediate or modulate synaptic scaling (Goddard et al., 2007; Rial Verde et al., 2006; Rutherford et al., 1998; Shepherd et al., 2006; Stellwagen and Malenka, 2006), including the Calcium/calmodulin-dependent protein kinases (CaMKs; Thiagarajan et al., 2005), but there is as yet no complete molecular pathway linking altered activity to homeostatic regulation of AMPAR accumulation. It also remains unclear which aspect of activity is sensed by neurons or networks during synaptic scaling: it has variously been proposed that neurons sense their own firing rate and globally scale synaptic weights up or down to compensate (Turrigiano and Nelson, 2004); that local changes in synaptic signaling induce local homeostatic changes in synaptic transmission at individual synapses (Sutton et al., 2006); or that synaptic scaling requires widespread changes in network activity, perhaps through activity-dependent release of a soluble factor by neurons or glia (Rutherford et al., 1998; Stellwagen and Malenka, 2006). To distinguish between these possibilities, we acutely blocked either a subset of presynaptic inputs or postsynaptic firing in individual neurons, while optically monitoring changes in synaptic strength over several hours. We find that cortical neurons homeostatically adjust synaptic strengths in response to changes in their own firing rate, through a pathway that involves changes in spike-mediated somatic calcium influx, CaMKIV signaling, and transcription.

## RESULTS

A major expression locus of synaptic scaling is postsynaptic changes in AMPAR accumulation. Previously, we showed that in cortical neurons, 1 to 2 days of TTX treatment increases endogenous GluR1 and GluR2 proportionally, and we used fluorescently tagged GluR2 to monitor the changes in synaptic strength induced by prolonged bath application of TTX (Wierenga et al., 2005). Here, we used time-lapse imaging to follow changes in GluR2 accumulation over the first few hours of activity blockade. Recombinant GluR2 was tagged with EYFP and when expressed in cultured cortical pyramidal neurons accumulated in dendritic puncta (Figure 1A), and these puncta colocalized with the excitatory synaptic marker PSD-95

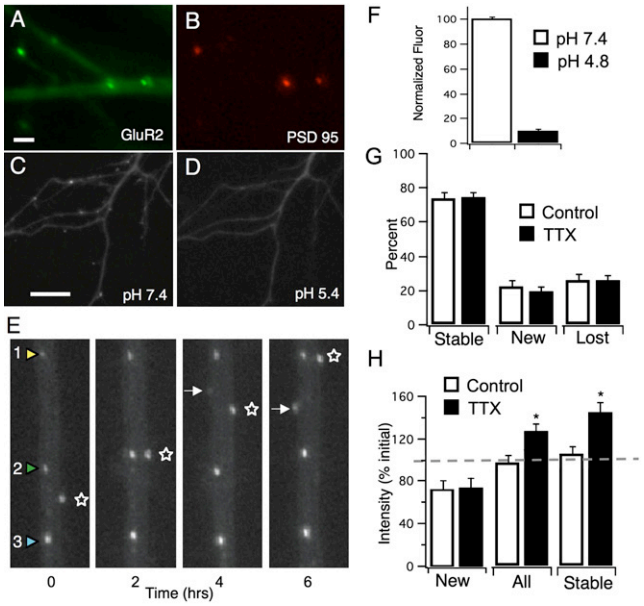


**Figure 1. Time-Lapse Imaging of Synaptic AMPA Receptor Fluorescence**

(A) Dendrite of pyramidal neuron transfected with GluR2-EYFP. Here and for all figures error bars represent SEM. Scale bar = 2 μm.

(B) GluR2-EYFP (A) colocalized with PSD-95-DsRed (B).

(C and D) GluR2-EYFP fluorescence at pH 7.4 (C) and immediately after washing into pH 5.4 medium (D). Scale bar = 10 μm.

(E) GluR2-EYFP imaged at 2 hr intervals, showing stable puncta (arrowheads 1, 2, 3), a mobile punctum (star), and a punctum that appeared de novo (while arrow). TTX was added to the bath after the first image.

(F) GluR2-EYFP fluorescence at low pH as a % of fluorescence at pH 7.4.

(G) Percent of stable puncta, puncta that appeared de novo (New), and puncta that disappeared (Lost) during the 4 hr imaging period, for control and TTX-treated neurons.

(H) Four hours of bath-applied TTX increased GluR2-EYFP intensity when averaged across all puncta (All) and stable puncta (Stable); control puncta intensity was unchanged. *TTX different from control, p = 0.001.

(Figure 1B; 93.5% ± 3.2% colocalization). Approximately 70% of these GluR2 puncta are also colocalized with the presynaptic marker synapsin and can recycle vesicles (Wierenga et al., 2005), suggesting that the majority of these GluR2 puncta represent functional synaptic sites.

GluR2 was tagged on the N terminal, so that when receptors are inserted into the plasma membrane the EYFP tag is on the extracellular surface. EYFP is highly pH sensitive (pKa of 7.0; Shaner et al., 2005), so tagged receptors localized in acidic intracellular compartments will have no appreciable fluorescence but when inserted into the plasma membrane (pH 7.4) will show strong fluorescence. Punctate GluR2-EYFP fluorescence was rapidly and reversibly quenched to 10% of control by low-pH medium (Figures 1C, 1D, and 1F), indicating that at least 90% is from surface receptors, and changes in this signal can be used as a noninvasive probe for changes in synaptic AMPAR accumulation. Repeated imaging of the same puncta revealed that the majority of GluR2 puncta (75%) were stable over 4 hr (Figure 1E, puncta 1, 2, 3; Figure 1G, Stable). The remaining puncta appeared de novo (Figure 1E, white arrow), disappeared during the imaging period, or were highly motile (Figure 1E, star). The fraction of puncta gained and lost were closely matched (Figure 1G, compare New to Lost), so that overall puncta number did not change significantly.

Synaptic scaling has been thought of as a process that operates over days (Turrigiano and Nelson, 2004). Surprisingly, we found that 4 hr of bath-applied TTX was sufficient to significantly increased GluR2 puncta intensity. Comparing all puncta (transient, stable, and new puncta; Figure 1H, All) with the effects only on stable puncta (Figure 1H, Stable) revealed that for both measures, control puncta intensity was stable over 4 hr, whereas puncta intensity significantly increased during TTX treatment. TTX had no effect on the proportion of stable and transient puncta (Figure 1G). Newly appeared puncta were weaker than average and similar in intensity for control and TTX (Figure 1H, New), suggesting that new puncta are not yet subject to the process that homeostatically regulates AMPAR number at more mature puncta. Below, we confined our analysis to puncta that persisted throughout the imaging experiment.

To examine the time course of TTX-induced AMPAR accumulation, we imaged neurons at 1 hr intervals for 4 hr (Figure 2A, top panel). There was no significant change in fluorescence under control conditions (Figure 2A, ctrl; 237 puncta from 10 neurons). In contrast, TTX induced a gradual increase in punctate GluR2 fluorescence, which was significant within 1 hr (Figure 2A, TTX; 164 puncta from 6 neurons). Synaptic scaling is bidirectional (Turrigiano et al., 1998); increasing activity with the $GABA_A$ receptor antagonist bicuculline significantly reduced synaptic AMPAR fluorescence (Figure 2A, bicucu; 153 puncta from 8 neurons). To verify that endogenous receptor levels are also rapidly affected by activity blockade, we used antibodies directed against an extracellular epitope of GluR2 under nonpermeant conditions to measure surface synaptic AMPAR levels in control and TTX-treated sister cultures, as described previously (Wierenga et al., 2005, 2006). TTX treatment for 4 hr significantly increased GluR2 intensity at synaptic sites (as defined by colocalization with synapsin); 24 hr of TTX further increased fluorescence (Figure 2B). TTX treatment did not affect colocolization between GluR2 and synapsin (control, 73% ± 3%; TTX 4 hr, 76% ± 3%; TTX 24 hr, 74% ± 4% colocalization). Taken together, these data indicate that modulating network activity rapidly and bidirectionally affects receptor trafficking to induce compensatory changes in AMPAR accumulation at putative synaptic sites.

The changes in AMPA accumulation measured above are more rapid than the changes in mEPSC amplitude we reported previously (Turrigiano et al., 1998). Since our culture conditions have changed since this first report (notably, we now plate neurons onto beds of glia), we compared the effects of 4 and 24 hr of TTX treatment on mEPSC amplitude. Surprisingly, 4–5 hr of TTX treatment was sufficient to produce a robust and significant increase in mEPSC amplitude, to approximately 130% of control values (Figures 2C–2F), in good agreement with our receptor accumulation data. Longer TTX treatment (24 hr) increased mEPSC amplitude further (Figure 2F), also in agreement with the receptor accumulation data (Figure 2B and Wierenga et al., 2005), but the rate of change is clearly faster during the first 4 hr than during the subsequent 20. The effects on mEPSCs induced by 4 hr of TTX were identical to those induced by longer TTX treatment, in that they occurred without

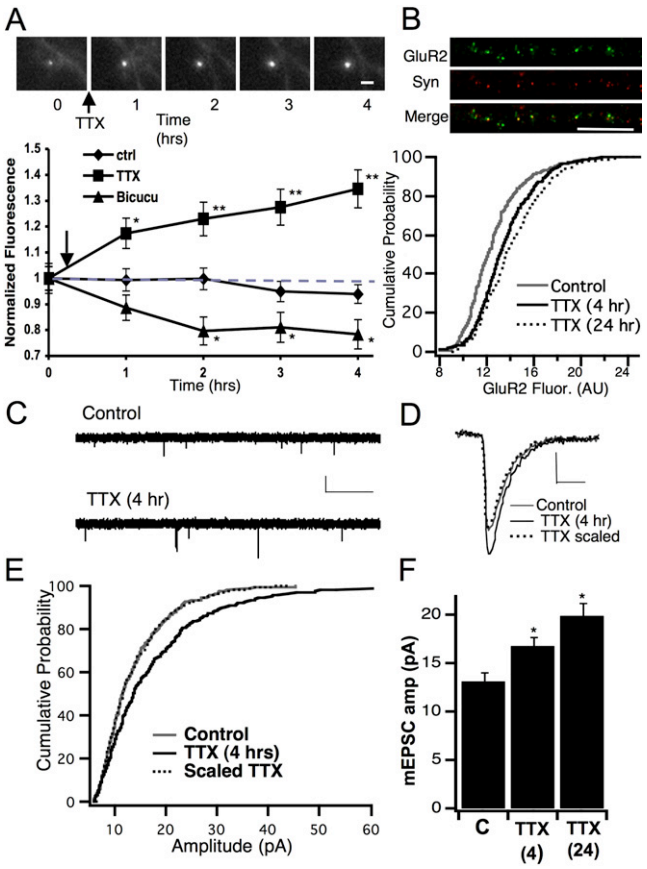


**Figure 2. Bath Application of TTX Rapidly Increased Synaptic AMPAR Accumulation and mEPSC Amplitude**

(A) Image sequence: GluR2-EYFP punctum imaged repeatedly over 4 hr; TTX was added to the bath at arrow. Scale bar = 2 μm. Plot: average punctate GluR2 fluorescence. Drugs (TTX or bicuculline) were added to the bath at arrow. *Drug different from control (ctrl), $p < 0.04$; **$p < 0.002$.

(B) TTX rapidly increased endogenous surface GluR2. Top: control dendrite stained against surface GluR2 and synapsin (Syn) and merged image (73% ± 3% colocalization). Bottom: cumulative histogram of GluR2 intensity for control (356 puncta from 19 neurons), 4 hr TTX (358 puncta from 19 neurons), and 24 hr TTX (360 puncta from 20 neurons). TTX (4 and 24 hr) was significantly different from control, $p < 0.001$.

(C) Example mEPSCs from a control neuron and neuron treated with TTX for 4 hr. Scale bar = 25 pA, 2 s.

(D) Average mEPSCs recorded for control and after 4 hr in TTX (n = 11 and 10). Dashed line indicates average mEPSC peak-scaled to control average.

(E) Cumulative histogram of mEPSC amplitude for control and TTX (4 hr). TTX distribution significantly different from control ($p = 0.006$); scaling down the TTX distribution (by a factor of 0.69) gave a good fit to the control distribution (scaled TTX and control not different, $p = 0.99$).

(F) Average mEPSC amplitude (n = 11, 10, and 10) for control, 4 hr TTX, and 24 hr TTX. *Different from control, $p < 0.03$, corrected t test.

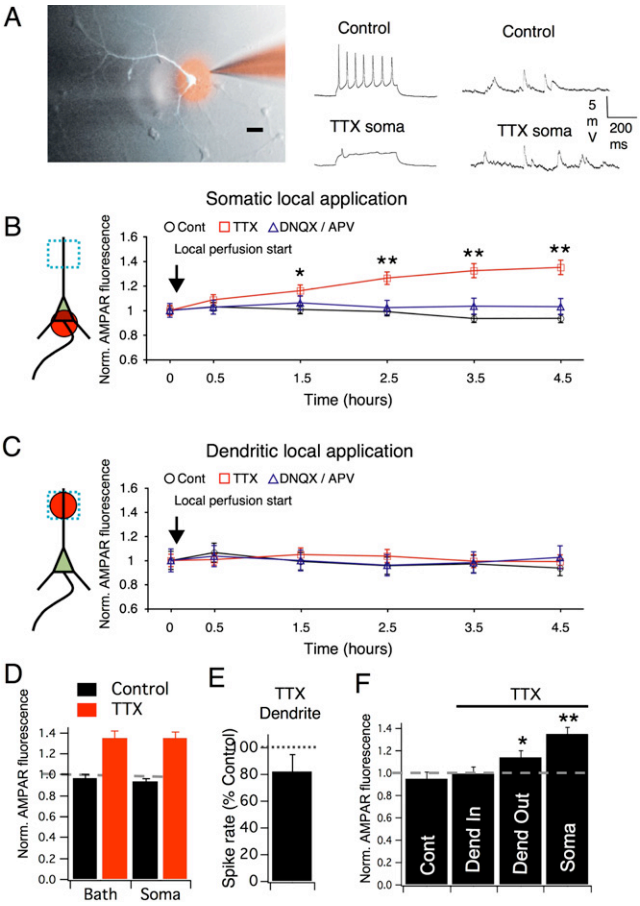


**Figure 3. Blockade of Somatic Spikes, but Not Local Synaptic Blockade, Increased Synaptic GluR2 Accumulation**

(A) Local perfusion. Overlaid fluorescence and DIC images showing transfected pyramidal neuron and perfusion pipettes (inflow on the right; outflow on the left). The fluorescent dye (red) shows the diameter of the perfusion spot. Scale bar = 20 μm. Middle panel: block of postsynaptic spikes by somatic perfusion of TTX. Top trace (Control) shows spikes elicited from a pyramidal neuron with a dc current injection, which are blocked when the local perfusion is moved onto the soma (TTX soma); synaptic potentials were not affected (right panel).

(B and C) Diagrams at left indicate perfusion (red circle) and measurement (blue box) sites during time-lapse imaging. (B) Somatic TTX significantly increased GluR2 fluorescence at dendritic puncta (red boxes). Control medium (black circles) or the AMPA and NMDA receptor antagonists DNQX/APV (blue triangles) had no significant effect. *$p < 0.01$; **$p < 0.001$ compared to perfusion of control medium. (C) Dendritic perfusion with control medium (circles), TTX (boxes), or DNQX/APV (triangles) had no effect on GluR2 accumulation at puncta within the perfusion spot.

(D) Bath-applied (Bath) and somatic TTX (Soma) increased GluR2 fluorescence to the same extent.

(E) Dendritic perfusion with TTX produced a small decrease in the firing rate of perfused neurons.

(F) Comparison of dendritic GluR2 fluorescence after somatic TTX perfusion (Soma) or for dendritic TTX perfusion for puncta inside (Dend In) and outside (Dend Out) the perfusion spot. *$p < 0.01$; **$p < 0.001$ compared to control.

any significant change in mEPSC kinetics (Figure 2D) or mEPSC frequency (TTX was 120% ± 10% of control values, $p = 0.46$), and TTX increased the amplitude distribution multiplicatively (Figure 2E; Turrigiano et al., 1998).

Bath-applied TTX could be affecting AMPAR accumulation by blocking postsynaptic firing, by reducing presynaptic release and/or local glutamate receptor activation, or by reducing network activity. To differentiate between these possibilities, we devised a perfusion system that allowed us to perfuse a local (approximately 30 μm diameter) region of the neuron with TTX to block somatic action potentials in individual neurons (Figure 3A).

Locally applying this perfusion spot to the soma blocked postsynaptic firing (Figure 3A, middle panel), while moving the pipette 30 μm away from the soma, or perfusing a region of dendrite, did not affect the ability of the neurons to fire during current injection (not shown). Synaptic input persisted during somatic perfusion with TTX (Figure 3A, left panel), and there was no difference in the integrated synaptic input before and during somatic TTX perfusion (TTX was 105% ± 6% of control, n = 5 neurons), indicating that blocking somatic spikes did not significantly reduce network activity.

Our strategy was to block postsynaptic firing with somatic TTX perfusion while monitoring the intensity of dendritic AMPAR puncta that were well outside the perfusion spot (at least 100 μm from the soma along the apical-like dendrite). Blocking somatic spikes in individual pyramidal neurons induced a gradual increase in dendritic punctate AMPAR fluorescence (Figure 3B; n = 199 puncta from 6 neurons). Somatic perfusion with control medium (Figure 3B; n = 201 puncta from 11 neurons) or with DNQX/APV (Figure 3B; n = 142 puncta from 5 neurons) had no effect. The magnitude (Figure 3D) and time course (compare Figures 3B and 2A) of the change in AMPAR accumulation induced by somatic spike blockade was similar to that induced by bath-applied TTX.

To determine whether locally blocking a subset of presynaptic inputs onto the dendrite is sufficient to induce a local increase in receptor fluorescence, we microperfused the apical-like dendrite with TTX and monitored AMPAR fluorescence at puncta within the perfusion spot (Figure 3C). Locally perfusing the dendrite with control medium induced no change in AMPAR fluorescence at perfused puncta (n = 99 puncta from 7 neurons), neither did perfusion with TTX (to block presynaptic spikes; n = 93 puncta from 10 neurons, p = 0.53 compared to perfusion with control medium) nor with DNQX/APV (to block postsynaptic glutamate receptors; n = 38 puncta from 4 neurons, p = 0.46). Thus, synaptic scaling cannot be induced locally in the dendrite but can be induced by a drop in postsynaptic activity.

TTX perfusion along the apical-like dendrite produced a small (approximately 20%) reduction in spontaneous firing of the perfused neuron (Figure 3E; n = 5 neurons), likely because this blocks a fraction of the synaptic inputs to the neuron. If synaptic scaling is a graded function of neuronal firing rate, then this reduction in firing should produce a small increase in AMPAR fluorescence, yet monitoring fluorescence within the perfusion spot showed no significant change in fluorescence (Figure 3C; Figure 3F, Dend In). To analyze this more thoroughly, we compared the fluorescence at dendritic puncta inside and outside the dendritic perfusion spot. Four hours of dendritic TTX perfusion produced a small but significant increase (approximately 14%) in AMPAR fluorescence at puncta outside the perfusion spot (Figure 3F, Dend Out). These data indicate that a graded drop in firing can increase dendritic AMPAR accumulation and suggest the presence of a competitive mechanism that prevents accumulation at locally blocked synapses.

Modeling studies have shown that an efficient way to design a homeostatic feedback loop is to use an integrator of intracellular calcium and adjust neuronal properties to keep this integrated calcium signal close to some "calcium set point" (LeMasson et al., 1993; Liu et al., 1998; Marder and Prinz, 2002). Somatic

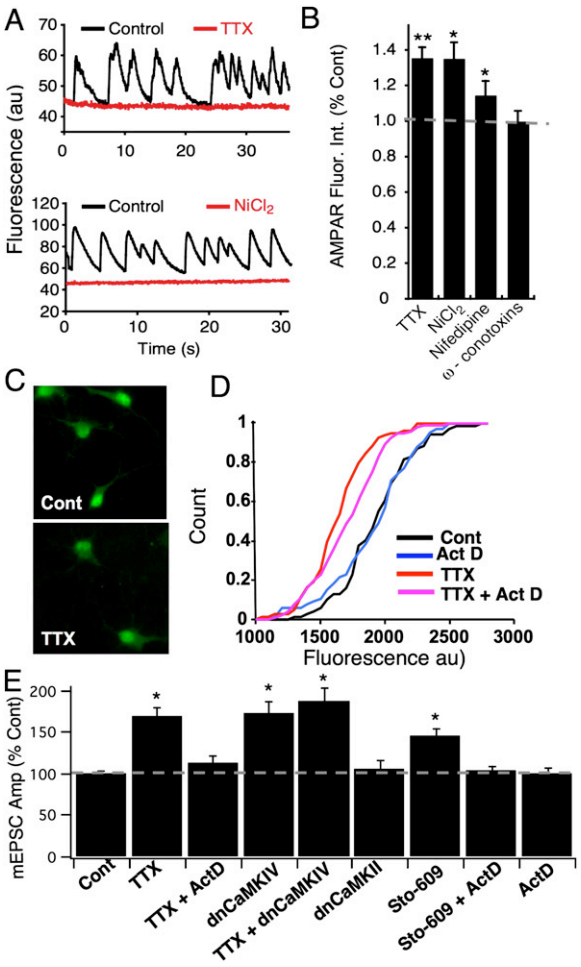


**Figure 4. Synaptic Scaling Was Induced by a Drop in Somatic Calcium, Reduced CaMKIV Activation, and Required Transcription**

(A) Top: somatic calcium transients before (black trace) and during (red trace) somatic perfusion with TTX. Bottom: somatic calcium transients before (black trace) and during (red trace) somatic perfusion with $NiCl_2$.

(B) Change in GluR2 fluorescence induced by 4 hr of somatic perfusion with TTX, nifedipine, or an ω-Conotoxins cocktail (to block P/Q and N channels). *Different from control, $p < 0.01$; **$p < 0.001$.

(C) Phospho-CaMKIV staining in control cultures (Cont) and cultures treated with TTX for 4 hr (TTX).

(D) Cumulative histogram of nuclear phospho-CaMKIV intensity for neurons treated for 4 hr with indicated agents; control, n = 69; TTX, n = 78; ActD, n = 65; TTX + ActD, n = 92. TTX was significantly different from control ($p = 0.01$), but not from TTX + ActD.

(E) mEPSC amplitude as % control for the conditions indicated, *$p < 0.05$, corrected t tests. From left to right, n = 25, 12, 12, 10, 10, 7, 9, 7, and 8.

spikes trigger somatic calcium transients that are blocked by local perfusion of TTX at the soma (Figure 4A, top panel), raising the possibility that blocking somatic spikes scales up synaptic strengths by reducing somatic calcium influx. To test this, we perfused the soma with $NiCl_2$, a broad-spectrum competitive blocker of calcium channels that completely abolished the somatic calcium transients (Figure 4A, bottom panel). We confirmed that perfusion with $NiCl_2$ did not affect the ability of the neurons to fire action potentials (data not shown). Somatic

perfusion with $NiCl_2$ induced a slow accumulation of AMPAR at dendritic puncta, similar in magnitude (Figure 4B) and time course (see Figure S1 available online) to that induced by somatic TTX perfusion. Perfusing the soma with the L type calcium channel blocker nifedipine produced a smaller but significant increase in AMPAR accumulation, while the N and P/Q type calcium channel blockers ω-Conotoxin GVIA and MVIIC had no effect (Figure 4B). Consistent with a partial effect of nifedipine on AMPAR accumulation, 24 hr of bath-applied nifedipine increased mEPSCs to values intermediate between control and TTX-treated cultures (nifedipine was 126% ± 11% of control, $p < 0.025$, $n = 9$; TTX was 154% ± 17% of control, $p < 0.01$, $n = 10$). Thus, a drop in somatic calcium influx, operating through a mixture of L type and other (possibly T or R type) calcium channels, generates a signal that leads to a gradual and cumulative increase in surface AMPAR at synaptic sites.

Calcium/calmodulin-dependent protein kinases (CaMKs) are important mediators of many forms of calcium-dependent plasticity (Lisman et al., 2002; Soderling, 1999). The CaMK inhibitor KN93 can induce homeostatic changes in synaptic function (Thiagarajan et al., 2005) but blocks all members of the CaMK family (CaMKI, CaMKII, and CaMKIV) with similar efficacy. Unlike CaMKII, CaMKIV has a predominantly somatic/nuclear localization (Nakamura et al., 1995; Soderling, 1999), raising the possibility that a drop in somatic calcium might induce synaptic scaling by reducing activation of nuclear CaMKIV. In keeping with published reports (Bito et al., 1996; Nakamura et al., 1995), staining against CaMKIV revealed a strong somatic/nuclear localization, with no appreciable signal within dendrites (Figure S2). A phospho-CaMKIV antibody (p-196, which detects the fully activated kinase) revealed strong levels of activated kinase in the nuclear compartment (Figure 4C), which was significantly reduced by 4 hr of TTX treatment (Figures 4C and 4D); baseline firing thus maintains a pool of CaMKIV in the activated state.

To directly test for a role of reduced CaMKIV signaling in the induction of synaptic scaling, we transfected neurons with a dominant-negative form of CaMKIV (dnCaMKIV, the kinase-dead mutation K75E; Chatila et al., 1996). Transfection with dnCaMKIV for 24 hr increased mEPSC amplitude to a similar extent as 24 hr of TTX (Figure 4E); further, the effects of dnCaMKIV and TTX occluded each other (Figure 4E, TTX + dnCaMKIV). Transfection with dnCaMKII (also kinase dead, K42M; Hanson et al., 1994) had no effect on mEPSC amplitude (Figure 4E, dnCaMKII). Unlike CaMKII, CaMKIV must be phosphorylated by CaM kinase kinase (CaMKK) for full activation (Soderling, 1999). Therefore, as a second means of inhibiting CaMKIV, we used the selective CaMKK inhibitor Sto-609 (Tokumitsu et al., 2002). Like dnCaMKIV, Sto-609 (bath applied for 4 hr) significantly increased mEPSC amplitude (Figure 4E) and synaptic accumulation of endogenous AMPAR (Figure S4). Taken together, these data strongly suggest that a drop in postsynaptic firing scales up mEPSC amplitude through a drop in somatic calcium influx and a subsequent reduction in CaMKIV signaling.

CaMKIV is a known transcriptional regulator (Soderling, 1999), and some forms of synaptic plasticity require gene expression for their induction or maintenance (West et al., 2002), but it is unknown whether synaptic scaling is transcription dependent. To determine whether changes in somatic calcium trigger synaptic scaling through a transcription-dependent pathway, we bath applied TTX along with the transcription inhibitor actinomycin D (ActD). Time-lapse imaging of synaptic GluR2-EYFP revealed that ActD completely blocked the increase in receptor accumulation normally induced by 4 hr of TTX (Figure S3); ActD also blocked the increase in endogenous AMPAR accumulation (Figure S4) and the increase in mEPSC amplitude induced by 4–5 hr of Sto-609 (Figure 4E, Sto-609 + ActD), as well as the increase in mEPSC amplitude induced by 24 hr of bath-applied TTX (Figure 4E, TTX + ActD). ActD had no significant effect on baseline transmission (Figure 4E, ActD), mEPSC frequency (ActD was 111.9% ± 21.3% of control), or on passive cellular properties such as input resistance (ActD was 97.0% ± 1.8% of control) and resting potential (ActD was 95.5% ± 12.5% of control). Scaling up of synaptic strengths thus depends upon transcription. ActD did not prevent the TTX-induced reduction in nuclear phospho-CaMKIV (Figure 4D), indicating that a drop in CaMKIV activation precedes transcription in the signaling pathway for synaptic scaling.

## DISCUSSION

Our data show that blocking postsynaptic firing in an individual cortical pyramidal neuron rapidly induces synaptic scaling, which is mediated through a drop in somatic calcium influx, a reduction in activation of CaMKIV, and a subsequent increase in gene transcription. In contrast, selectively blocking a subset of presynaptic inputs did not induce scaling at the blocked synapses, demonstrating that purely local changes in either presynaptic firing or postsynaptic receptor activation are not sufficient to induce local homeostatic changes in synaptic strength. Cortical neurons thus use a somatically activated, calcium- and CaMKIV-dependent transcriptional mechanism to adaptively increase synaptic strengths in response to a reduction in their own firing.

The standard paradigms for inducing postsynaptically expressed synaptic scaling, including blockade or enhancement of network activity in culture and sensory deprivation in the intact animal, modify the activity of the entire network. Consequently, the identity of the activity signal that triggers synaptic scaling has been a matter of speculation. At the invertebrate NMJ and in hippocampal cultures, chronic hyperpolarization of individual neurons or muscle fibers through expression of an inwardly rectifying K channel can induce a presynaptic form of homeostatic plasticity (Murthy et al., 2001; Paradis et al., 2001), but because this manipulation hyperpolarizes both somatic and dendritic regions of the neuron, it cannot distinguish between a critical role for somatic versus local dendritic depolarization in the induction of homeostatic plasticity. To circumvent this problem, here we used acute pharmacological blockade of postsynaptic firing (without concomitant hyperpolarization) in individual neurons and found that this was sufficient to induce postsynaptically expressed synaptic scaling. The effects of somatic block of spikes and of global block of network activity with TTX were similar, strongly suggesting that blocking network activity has no effects on synaptic scaling over and above blocking postsynaptic spikes. It has recently been reported that synaptic scaling induced by 48 hr of activity blockade requires

release of the cytokine TNF-alpha from glia (Stellwagen and Malenka, 2006). Our data do not rule out a role for non-cell-autonomous neuron-glial signaling in the early phases of synaptic scaling but argue that any such signaling must be triggered by changes in somatic calcium influx in individual neurons.

In contrast to the effects of blocking postsynaptic firing, acute pharmacological blockade of either presynaptic release or postsynaptic receptor activation at a subset of neocortical synapses did not affect the accumulation of GluR2 locally at the blocked synapses. This result is in agreement with two recent studies showing that genetic block of presynaptic release at a subset of synapses (leaving others active) does not locally increase GluR1 or GluR2 accumulation and in fact can reduce AMPAR levels relative to nearby unblocked synapse (Harms et al., 2005; Ehlers et al., 2007). Interestingly, when TTX was first bath applied for several hours and then receptors were locally blocked in hippocampal neurons, there was a local acceleration of GluR1 accumulation (Sutton et al., 2006). Taken together with these other studies, our data suggest that local synaptic blockade is not sufficient to locally increase AMPAR accumulation but may accelerate it when combined with global activity blockade.

The roles of CaMKIV in synaptic function are only poorly understood. Genetic manipulations of CaMKIV signaling has suggested a role in the maintenance of LTP (Ho et al., 2000; Kang et al., 2001), BDNF-induced synaptic potentiation (Minichiello et al., 2002), and cerebellar LTD and motor learning (Boyden et al., 2006; Ho et al., 2000), suggesting that CaMKIV signaling can promote or maintain either increases or decreases in synaptic strength depending on the cell type. Our data suggest that, in neocortical neurons, a drop in somatic calcium influx is sensed through a drop in activated nuclear CaMKIV, which then triggers a homeostatic increase in synaptic AMPAR accumulation and mEPSC amplitude. In apparent contrast to our results, dnCaMKIV had little effect on evoked transmission in hippocampal CA1 neurons (Marie et al., 2005); mEPSCs were not assessed in this study so it is not clear whether this difference is methodological or reflects differences in baseline levels of activated CaMKIV or other cell-type-specific differences in CaMKIV function. Our data do not address whether scaling down of synaptic strengths in response to increased activity is mediated through CaMKIV signaling. Overexpression of a truncated constitutively active CaMKIV was observed to increase evoked transmission in hippocampal CA1 (Marie et al., 2005), a change which is opposite in sign from that predicted if increased CaMKIV signaling mediates homeostatic scaling down of synaptic strengths. However, ectopically expressed CaMKIV is strongly localized to the cytoplasmic compartment (Matthews et al., 1994), whereas endogenous activated CaMKIV is largely confined to the nucleus (Bito et al., 1996; Nakamura et al., 1995; Soderling, 1999). Overexpressed constitutively active CaMKIV will thus have access to targets normally unavailable to the endogenous kinase, and is unlikely to mimic the effects of endogenous CaMKIV activation.

Synaptic scaling is a cumulative, dynamic, and reversible form of synaptic plasticity, so it was surprising to find that even the early stages of scaling (within the first 4 hr) are transcription dependent. Activity blockade appears to rapidly upregulate the expression of a protein or proteins that are necessary for increasing the accumulation of AMPARs. This dependence on transcription is in contrast to rapid presynaptic homeostatic changes at the *Drosophila* NMJ, which occur within minutes and do not require transcription (Frank et al., 2006). CaMKIV is a known transcriptional regulator and can target CREB, CBP, and likely a large number of other genes, transcription factors, and regulators of alternative splicing (Bito et al., 1996; Soderling, 1999). Recently, it has been suggested that the immediate-early gene Arc is involved in synaptic scaling (Rial Verde et al., 2006; Shepherd et al., 2006). However, changes in Arc expression cannot account for the transcriptional requirement reported here, because unlike immediate-early genes such as Arc whose transcription is induced by activity, scaling up of synaptic strengths requires a factor or factors whose transcription is increased by activity blockade.

How synaptic scaling will function within in vivo networks and interact with other forms of synaptic plasticity depends critically on how it is induced. Locally induced scaling would tend to erase or reverse synaptic changes produced by long-term depression (or potentiation), because when a synapse is weakened (or strengthened) it will generate less (or more) local dendritic activation, and this would cause the synapse to be locally scaled up (or down) in strength again. Such a local process could contribute to the stabilization of neuronal activity (Rabinowitch and Segev, 2006) but would do so at the expense of efficient information storage. Our data argue against such an exclusively local mechanism and instead lend strong support to the idea that cortical neurons globally adjust synaptic strengths in response to changes in their own firing rates. Such a mechanism has the computational advantage of efficiently normalizing synaptic strengths without interfering with the ability of Hebbian plasticity mechanisms to store information (Abbott and Nelson, 2000; Miller, 1996; Turrigiano and Nelson, 2004).

## EXPERIMENTAL PROCEDURES

Dissociated neuronal cultures were prepared from P3 Long-Evans rat pups, and immunohistochemistry and electrophysiology were performed as described previously (Pratt et al., 2003; Wierenga et al., 2005). Cultures were transfected 24 hr prior to experimentation using Lipofectamine and were used after 7–10 DIV. Time-lapse imaging (for details, local perfusion technique, and pharmacology see Supplemental Experimental Procedures) was as follows: cultures were perfused with imaging medium at 35°C and viewed on an inverted Olympus IX70 microscope with a 60× oil immersion objective (n.a.1.25) using 3% neutral density filters. Digital images were acquired with an Orca ER cooled CCD camera, captured using Openlab, and analyzed using ImageJ. Data were expressed as punctum/local dendrite intensity. Statistics: values are mean ± standard error of the mean for the number of neurons (or puncta) indicated. Statistics were performed using two-tailed unpaired Student's t tests, corrected for multiple comparisons using a Bonferroni correction factor. For comparisons of cumulative distributions, a Kolmogorov-Smirnov (KS) test was used. A p value of $<0.05$ was considered statistically significant.

## SUPPLEMENTAL DATA

The Supplemental Data for this article can be found online at http://www.neuron.org/cgi/content/full/57/6/819/DC1/.

## ACKNOWLEDGMENTS

This work was supported by NIH grant NS 36853 and NSF grant IBN 023519.

Received: November 29, 2006
Revised: April 27, 2007
Accepted: February 29, 2008
Published: March 26, 2008

## REFERENCES

Abbott, L.F., and Nelson, S.B. (2000). Synaptic plasticity: taming the beast. Nat. Neurosci. *3*, 1178–1183.

Bito, H., Deisseroth, K., and Tsien, R.W. (1996). CREB phosphorylation and dephosphorylation: a Ca(2+)- and stimulus duration-dependent switch for hippocampal gene expression. Cell *87*, 1203–1214.

Boyden, E.S., Katoh, A., Pyle, J.L., Chatila, T.A., Tsien, R.W., and Raymond, J.L. (2006). Selective engagement of plasticity mechanisms for motor memory storage. Neuron *51*, 823–834.

Burrone, J., and Murthy, V.N. (2003). Synaptic gain control and homeostasis. Curr. Opin. Neurobiol. *13*, 560–567.

Chatila, T., Anderson, K.A., Ho, N., and Means, A.R. (1996). A unique phosphorylation-dependent mechanism for the activation of Ca2+/calmodulin-dependent protein kinase type IV/GR. J. Biol. Chem. *271*, 21542–21548.

Desai, N.S., Cudmore, R.H., Nelson, S.B., and Turrigiano, G.G. (2002). Critical periods for experience-dependent synaptic scaling in visual cortex. Nat. Neurosci. *5*, 783–789.

Ehlers, M.D., Heine, M., Groc, L., Lee, M.C., and Choquet, D. (2007). Diffusional trapping of GluR1 AMPA receptors by input-specific synaptic activity. Neuron *54*, 447–460.

Frank, C.A., Kennedy, M.J., Goold, C.P., Marek, K.W., and Davis, G.W. (2006). Mechanisms underlying the rapid induction and sustained expression of synaptic homeostasis. Neuron *52*, 663–677.

Goddard, C.A., Butts, D.A., and Shatz, C.J. (2007). Regulation of CNS synapses by neuronal MHC class 1. Proc. Natl. Acad. Sci. USA *104*, 6828–6833.

Goel, A., Jiang, B., Xu, L.W., Song, L., Kirkwood, A., and Lee, H.K. (2006). Cross-modal regulation of synaptic AMPA receptors in primary sensory cortices by visual experience. Nat. Neurosci. *9*, 1001–1003.

Grunwald, M.E., Mellem, J.E., Strutz, N., Maricq, A.V., and Kaplan, J.M. (2004). Clathrin-mediated endocytosis is required for compensatory regulation of GLR-1 glutamate receptors after activity blockade. Proc. Natl. Acad. Sci. USA *101*, 3190–3195.

Hanson, P.I., Meyer, T., Stryer, L., and Schulman, H. (1994). Dual role of calmodulin in autophosphorylation of multifunctional CaM kinase may underlie decoding of calcium signals. Neuron *12*, 943–956.

Harms, K.J., Tovar, K.R., and Craig, A.M. (2005). Synapse-specific regulation of AMPA receptor subunit composition by activity. J. Neurosci. *25*, 6379–6388.

Ho, N., Liauw, J.A., Blaeser, F., Wei, F., Hanissian, S., Muglia, L.M., Wozniak, D.F., Nardi, A., Arvin, K.L., Holtzman, D.M., et al. (2000). Impaired synaptic plasticity and cAMP response element-binding protein activation in Ca2+/calmodulin-dependent protein kinase type IV/Gr-deficient mice. J. Neurosci. *20*, 6459–6472.

Ju, W., Morishita, W., Tsui, J., Gaietta, G., Deerinck, T.J., Adams, S.R., Garner, C.C., Tsien, R.Y., Ellisman, M.H., and Malenka, R.C. (2004). Activity-dependent regulation of dendritic synthesis and trafficking of AMPA receptors. Nat. Neurosci. *7*, 244–253.

Kang, H., Sun, L.D., Atkins, C.M., Soderling, T.R., Wilson, M.A., and Tonegawa, S. (2001). An important role of neural activity-dependent CaMKIV signaling in the consolidation of long-term memory. Cell *106*, 771–783.

LeMasson, G., Marder, E., and Abbott, L.F. (1993). Activity-dependent regulation of conductances in model neurons. Science *259*, 1915–1917.

Lisman, J., Schulman, H., and Cline, H. (2002). The molecular basis of CaMKII function in synaptic and behavioural memory. Nat. Rev. Neurosci. *3*, 175–190.

Lissin, D.V., Gomperts, S.N., Carroll, R.C., Christine, C.W., Kalman, D., Kitamura, M., Hardy, S., Nicoll, R.A., Malenka, R.C., and von Zastrow, M. (1998). Activity differentially regulates the surface expression of synaptic AMPA and NMDA glutamate receptors. Proc. Natl. Acad. Sci. USA *95*, 7097–7102.

Liu, Z., Golowasch, J., Marder, E., and Abbott, L.F. (1998). A model neuron with activity-dependent conductances regulated by multiple calcium sensors. J. Neurosci. *18*, 2309–2320.

Maffei, A., Nelson, S.B., and Turrigiano, G.G. (2004). Selective reconfiguration of layer 4 visual cortical circuitry by visual deprivation. Nat. Neurosci. *7*, 1353–1359.

Malenka, R.C., and Bear, M.F. (2004). LTP and LTD: An embarrassment of riches. Neuron *44*, 5–21.

Marder, E., and Prinz, A.A. (2002). Modeling stability in neuron and network function: the role of activity in homeostasis. Bioessays *24*, 1145–1154.

Marie, H., Morishita, W., Yu, X., Calakos, N., and Malenka, R.C. (2005). Generation of silent synapses by acute in vivo expression of CaMKIV and CREB. Neuron *45*, 741–752.

Matthews, R.P., Guthrie, C.R., Wailes, L.M., Zhao, X., Means, A.R., and McKnight, G.S. (1994). Calcium/calmodulin-dependent protein kinase types II and IV differentially regulate CREB-dependent gene expression. Mol. Cell. Biol. *14*, 6107–6116.

Miller, K.D. (1996). Synaptic economics: Competition and cooperation in synaptic plasticity. Neuron *17*, 371–374.

Minichiello, L., Calella, A.M., Medina, D.L., Bonhoeffer, T., Klein, R., and Korte, M. (2002). Mechanism of TrkB-mediated hippocampal long-term potentiation. Neuron *36*, 121–137.

Murthy, V.N., Schikorski, T., Stevens, C.F., and Zhu, Y. (2001). Inactivity produces increases in neurotransmitter release and synapse size. Neuron *32*, 673–682.

Nakamura, Y., Okuno, S., Sato, F., and Fujisawa, H. (1995). An immunohistochemical study of Ca2+/calmodulin-dependent protein kinase IV in the rat central nervous system: light and electron microscopic observations. Neuroscience *68*, 181–194.

O'Brien, R.J., Kamboj, S., Ehlers, M.D., Rosen, K.R., Fischbach, G.D., and Huganir, R.L. (1998). Activity-dependent modulation of synaptic AMPA receptor accumulation. Neuron *21*, 1067–1078.

Paradis, S., Sweeney, S.T., and Davis, G.W. (2001). Homeostatic control of presynaptic release is triggered by postsynaptic membrane depolarization. Neuron *30*, 737–749.

Pratt, K.G., Watt, A.J., Griffith, L.C., Nelson, S.B., and Turrigiano, G.G. (2003). Activity-dependent remodeling of presynaptic inputs by postsynaptic expression of activated CaMKII. Neuron *39*, 269–281.

Rabinowitch, I., and Segev, I. (2006). The interplay between homeostatic synaptic plasticity and functional dendritic compartments. J. Neurophysiol. *96*, 276–283.

Rial Verde, E.M., Lee-Osbourne, J., Worley, P.F., Malinow, R., and Cline, H.T. (2006). Increased expression of the immediate-early gene arc/arg3.1 reduces AMPA receptor-mediated synaptic transmission. Neuron *52*, 461–474.

Rutherford, L.C., Nelson, S.B., and Turrigiano, G.G. (1998). BDNF has opposite effects on the quantal amplitude of pyramidal neuron and interneuron excitatory synapses. Neuron *21*, 521–530.

Shaner, N.C., Steinbach, P.A., and Tsien, R.Y. (2005). A guide to choosing fluorescent proteins. Nat. Methods *2*, 905–909.

Shepherd, J.D., Rumbaugh, G., Wu, J., Chowdhury, S., Plath, N., Kuhl, D., Huganir, R.L., and Worley, P.F. (2006). Arc/Arg3.1 mediates homeostatic synaptic scaling of AMPA receptors. Neuron *52*, 475–484.

Soderling, T.R. (1999). The Ca-calmodulin-dependent protein kinase cascade. Trends Biochem. Sci. *24*, 232–236.

Stellwagen, D., and Malenka, R.C. (2006). Synaptic scaling mediated by glial TNF-alpha. Nature *440*, 1054–1059.

Sutton, M.A., Ito, H.T., Cressy, P., Kempf, C., Woo, J.C., and Schuman, E.M. (2006). Miniature neurotransmission stabilizes synaptic function via tonic suppression of local dendritic protein synthesis. Cell *125*, 785–799.

Thiagarajan, T.C., Lindskog, M., and Tsien, R.W. (2005). Adaptation to synaptic inactivity in hippocampal neurons. Neuron *47*, 725–737.

Tokumitsu, H., Inuzuka, H., Ishikawa, Y., Ikeda, M., Saji, I., and Kobayashi, R. (2002). STO-609, a specific inhibitor of the Ca(2+)/calmodulin-dependent protein kinase kinase. J. Biol. Chem. *277*, 15813–15818.

Turrigiano, G.G., and Nelson, S.B. (2004). Homeostatic plasticity in the developing nervous system. Nat. Rev. Neurosci. *5*, 97–107.

Turrigiano, G.G., Leslie, K.R., Desai, N.S., Rutherford, L.C., and Nelson, S.B. (1998). Activity-dependent scaling of quantal amplitude in neocortical neurons. Nature *391*, 892–896.

West, A.E., Griffith, E.C., and Greenberg, M.E. (2002). Regulation of transcription factors by neuronal activity. Nat. Rev. Neurosci. *3*, 921–931.

Wierenga, C.J., Ibata, K., and Turrigiano, G.G. (2005). Postsynaptic expression of homeostatic plasticity at neocortical synapses. J. Neurosci. *25*, 2895–2905.

Wierenga, C.J., Walsh, M.F., and Turrigiano, G.G. (2006). Temporal regulation of the expression locus of homeostatic plasticity. J. Neurophysiol. *96*, 2127–2133.